Energy Conversion and Management 53 (2012) 55–67

Contents lists available at SciVerse ScienceDirect

Energy Conversion and Management

journal homepage: www.elsevier.com/locate/enconman

Comparison among nonlinear excitation control strategies used for damping power system oscillations

A.E. Leon [a,*], J.A. Solsona [a], M.I. Valla [b]

[a] Instituto de Investigaciones en Ingeniería Eléctrica (IIIE) "Alfredo Desages", Universidad Nacional del Sur (DIEC-UNS), Avenida Alem 1253, Bahía Blanca 8000, Argentina
[b] Laboratorio de Electrónica Industrial, Control e Instrumentación (LEICI), Departamento de Electrotecnia, Facultad de Ingeniería, Universidad Nacional de La Plata (UNLP) and CONICET, La Plata 1900, Argentina

ARTICLE INFO

Article history:
Received 16 June 2010
Received in revised form 10 August 2011
Accepted 11 August 2011

Keywords:
Damping oscillations
Nonlinear excitation control
Power systems
Transient stability
Voltage regulation

ABSTRACT

This work is focused on the problem of power system stability. A thorough description of nonlinear control strategies for synchronous generator excitation, which are designed for damping oscillations and improving transient stability on power systems, is presented along with a detailed comparison among these modern strategies and current solutions based on power system stabilizers. The performance related to damping injection in each controller, critical time enhancement, robustness against parametric uncertainties, and control signal energy consumption is analyzed. Several tests are presented to validate discussions on various advantages and disadvantages of each control strategy.

1. Introduction

Current power systems are in a stage of great change due to the introduction of new technologies based on power electronics [1–5]. Also, several flexible alternating current transmission systems (FACTS) [6–8] (*e.g.* static synchronous compensators [9,10], static synchronous series compensators [11], unified power flow controllers [12], and high-voltage direct current transmissions [13–15]) are being installed in the power grid, as well as alternative energy sources such as wind energy conversion systems, and photo-voltaic generation systems. Moreover, there are projections which indicate a remarkable growth in this kind of energy sources in future power systems [16–23]. In many power networks there are great distances between the places where energy is generated and consumed. This makes groups of generators behave like areas, and that oscillations among them might produce great blackouts [24,25]. Besides, with the aim of transporting a greater amount of power, it is usual to work to the limit of the power system stability. In this complex framework, energy quality standards are more and more demanding. Because of what has been already stated, it is compelling to find solutions for guaranteeing stability in current and future power systems. For this reason, many control strategies have been presented to damp oscillations. Power systems can be stabilized either by including FACTS which control the power flow and regulate the voltage level, or by controlling the excitation of synchronous generators. This work is mainly focused on the latter approach. Although the excitation control solution is, from an economical point of view, more viable because it uses the existing facilities in the generating stations, the design of this kind of excitation controllers is not trivial due to the nonlinear nature of the generator model.

One of the first studies on stabilization via generator excitation was reported in [26]. It was shown there that power system stabilizers (PSS) are able to damp oscillations through a stabilizing signal included in the excitation system. PSSs are built via robust transfer functions and tuned via small-signal techniques. However, the operation point of a power system can be modified by several disturbances, such as short circuits and changes on the network topology, producing stability problems which cannot be overcome with PSS controllers. For this reason, to enhance performance throughout the whole operation range and in the presence of great disturbances, a series of works on nonlinear controller design were presented in the 1990s [27–30], and recently [31,32]. These works were based on feedback linearization (FL), a strategy which is able to cancel the model nonlinearities to obtain an input–output linear dynamics. Some approaches based on Lyapunov theory (named L_gV control), which improves the system damping through excitation control, were presented in [33]. An excitation control via interconnection and damping assignment (IDA) based on the criteria of energy shaping through a physical approach of the problem was

* Corresponding author. Tel.: +54 291 459 5101x3338; fax: +54 291 459 5154.
E-mail addresses: aleon@ymail.com (A.E. Leon), jsolsona@uns.edu.ar (J.A. Solsona), mvalla@ing.unlp.edu.ar (M.I. Valla).

0196-8904/$ - see front matter © 2011 Elsevier Ltd. All rights reserved.
doi:10.1016/j.enconman.2011.08.010

treated in [34,35]. Sliding-mode, backstepping and H_∞ control techniques were applied in [36–40], respectively. In the near future, with the arrival of smart grids, these excitation controllers will work in coordination with the above-mentioned FACTS to enhance the stabilizing capacity of the power systems against great disturbances on the electric network.

The referred works are focused on generator excitation control, and compare their proposals with current PSSs, but they rarely show comparisons among nonlinear control strategies. Besides, all of these nonlinear strategies are techniques in development, and their practical implementations, robustness and performance are in discussion. For these reasons, the performance of nonlinear control strategies found in the literature for damping power system oscillation is compared in this work. The controllers selected for such comparison are FL, IDA, L_gV, and their linear counterpart PSS, analyzing the performance of each one against short circuits on the grid, evaluating the energy contained in the control signal generated by them, and studying their sensitivity to uncertainties in the system parameters.

Finally, we can remark three main contributions of this work. First, a comparison among nonlinear controllers for synchronous generators is accomplished; articles which present new nonlinear controllers rarely confront their proposals with other nonlinear controllers, or limit the comparison to linear schemes. Second, a throughout description of nonlinear controllers for both angle transient stability and post-fault voltage regulation issues is developed. Besides, it is presented several advantages and disadvantages of each control strategy related with damping injection performance, critical time enhancement, robustness against parametric uncertainties, control energy consumption and multimachine scenarios. Third, unlike to what has been discussed by other researchers, we show that FL and IDA controllers have many points in common. Moreover, we find a particular selection of the IDA gain to achieve the same performance of that of the FL control by considering the IDA gain as a state dependent parameter.

This work is organized as follows: equations describing the synchronous generator are presented in Section 2; the different control strategies to be contrasted are introduced in Section 3 in Section 4, a description of several methods to achieve the generator voltage regulation is developed; Section 5 assesses the performance of the strategies against disturbances, analyzing robustness to parameter variations and multimachine tests. A link between FL and IDA controllers is shown in Section 6. Conclusions are presented in Section 7.

2. Synchronous generator modeling

Synchronous generator model is complex because it presents coupling of many windings, becoming a high-order and strongly coupled model. A synchronous generator schematic representation is shown in Fig. 1. It can be seen there, the three stator windings representing the phases (a,b,c), four rotor circuits which model the field winding (F), the two damper windings (D,Q), and also a winding (G) which models the closed circuits through which the Foucault currents circulate in solid rotors (for instance, in turbogenerators). However, in stability studies and for control purposes, it is usual to work just with a transient model of the generator, assuming that in this period the effect of the damper windings has vanished, and that their dynamics can be either eliminated or simply replaced by a proportional term to the speed deviation. This transient model is widely used on power system control literature [27–29,32–35,38,41], and it has proved to produce very good results. The elimination of the damper winding dynamics is also justified, as they can be interpreted as elements which produce a nonlinear damping on the generator. Consequently, including

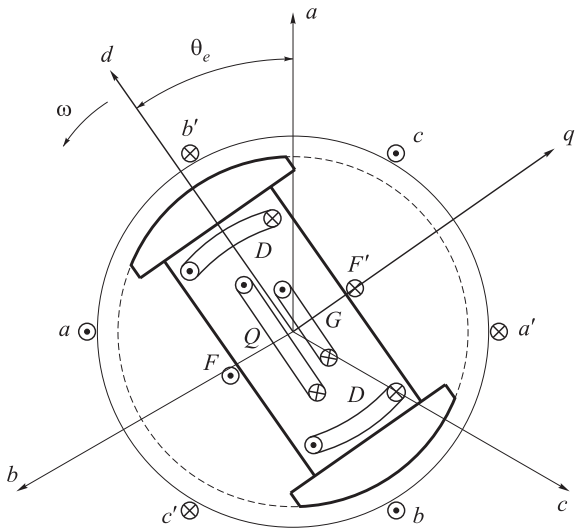

Fig. 1. Synchronous generator representation.

them in the controller design and trying to cancel their effect would not be beneficial, since this would lead to the implementation of a more complex control law. Besides, in this kind of oscillation studies about 1 Hz, stator winding dynamics is considered as algebraic because its oscillation frequency is much higher than mechanical and rotor winding dynamics. Therefore, the model considered in generators for the controller design is the classical transient model in a dq synchronous reference frame [42],

$$\dot{\delta} = \Delta\omega, \tag{1}$$

$$2H\Delta\dot{\omega} = P_m - \frac{V_r E'_q}{X'_d + X_E}\sin\delta - K_d\Delta\omega, \tag{2}$$

$$T'_{d0}\dot{E}'_q = \frac{(X_d - X'_d)}{(X'_d + X_E)}V_r\cos\delta - \frac{(X_d + X_E)}{(X'_d + X_E)}E'_q + E^0_{fd} + T'_{d0}u, \tag{3}$$

where δ, $\Delta\omega$, and E'_q are state variables representing the load angle, the speed deviation, and the transient ElectroMotive Force (EMF) voltage in the quadrature axis, respectively. The input control will be u, representing the additional voltage which is added to the constant field voltage E^0_{fd}. P_m is the turbine mechanical power, which is considered to be a constant because it is associated with very slow time constants. Definitions of the rest of parameters and their values can be consulted in Table 1. In a more compact notation, the model (1)–(3) results,

$$\dot{\mathbf{x}} = \mathbf{f}(\mathbf{x}) + \mathbf{g}u, \tag{4}$$

with,

$$\mathbf{f}(\mathbf{x}) \triangleq \begin{bmatrix} x_2 \\ -b_1 x_3 \sin x_1 - b_2 x_2 + P \\ b_3 \cos x_1 - b_4 x_3 + E \end{bmatrix}, \tag{5}$$

$$\mathbf{g} \triangleq [0 \quad 0 \quad 1]^T, \tag{6}$$

where x_i, b_i, P and E are defined as follows:

$$\begin{aligned} &x_1 \triangleq \delta, && b_1 \triangleq \tfrac{V_r}{2H(X'_d+X_E)}, && b_2 \triangleq \tfrac{K_d}{2H}, \\ &x_2 \triangleq \Delta\omega, && b_3 \triangleq \tfrac{(X_d-X'_d)V_r}{T'_{d0}(X'_d+X_E)}, && b_4 \triangleq \tfrac{(X_d+X_E)}{T'_{d0}(X'_d+X_E)}, \\ &x_3 \triangleq E'_q, && P \triangleq \tfrac{P_m}{2H}, && E \triangleq \tfrac{E^0_{fd}}{T'_{d0}}. \end{aligned} \tag{7}$$

The following system should be solved in order to calculate the equilibrium point (named $\mathbf{x}^\star$) of the system (4),

Table 1
Data and parameter values.

Description	Parameter	Value
Power system		
Rated power (MVA)	S_N	4×555
Base angular frequency (r/s)	Ω_B	$2\pi 60$
Inertia constant (s)	H	3.5
D-axis reactance	X_d	1.81
D-axis transient reactance	X'_d	0.3
External reactance	X_E	0.4752
D-axis transient open circuit time constant (s)	T'_{d0}	8.0
Infinite bus voltage	V_r	0.90081
Mechanical power	P_m	0.9
Equilibrium exciter voltage	E^0_{fd}	1.78
Maximum exciter voltage	$E^{\max}_{fd}$	7.0
Minimum exciter voltage	$E^{\min}_{fd}$	−6.4
FL control		
γ_1 design gain	γ_1	105
γ_2 design gain	γ_2	517
γ_3 design gain	γ_3	1225
IDA control		
Interconnection injection gain	α_1 $(=-b_1/\alpha_2)$	−0.6
α_2 design gain	α_2 $(=b_1 b_4/b_3)$	105
Damping injection gain	k_v	0.07
PSS control		
Amplifier stage gain	K_A	200
Amplifier stage time constant (s)	T_A	0.0001
Power system stabilizer gain	K_S	9.5
Washout time constant (s)	T_{wo}	1.41
Phase compensation time constant (s)	T_1	0.154
Phase compensation time constant (s)	T_2	0.033
Phase compensation time constant (s)	$T_3 = T_4$	1.0
Stabilizer output limits	$V^{\min,\max}_{ST}$	±0.2

All parameters are in per unit on a base of 2220 MVA, and 24 kV, except the indicated within parentheses.

$$0 = x_2^\star, \tag{8}$$
$$0 = -b_1 x_3^\star \sin x_1^\star - b_2 x_2^\star + P, \tag{9}$$
$$0 = b_3 \cos x_1^\star - b_4 x_3^\star + E + u, \tag{10}$$

or, in a simpler way, solving the equilibrium $\mathbf{x}^\star = \begin{bmatrix} x_1^\star & 0 & x_3^\star \end{bmatrix}^T$ from,

$$P = b_1 x_3^\star \sin x_1^\star, \tag{11}$$
$$E = b_4 x_3^\star - b_3 \cos x_1^\star. \tag{12}$$

If $E > \frac{b_4 P}{b_1} - b_3$, then $\mathbf{x}^\star$will be an asymptotically stable equilibrium point (see [43] for further details).

For this model, the equilibrium point of (4) is locally stable with Lyapunov function given by [34],

$$H(\mathbf{x}) = \frac{1}{2}x_2^2 + b_1 x_3 (\cos x_1^\star - \cos x_1) - P(x_1 - x_1^\star) + \frac{b_1 b_4}{2 b_3}(x_3 - x_3^\star)^2. \tag{13}$$

Therefore, the system (4) rewritten in a port-controlled hamiltonian (PCH) structure becomes,

$$\dot{\mathbf{x}} = [\mathbf{J} - \mathbf{R}] \frac{\partial H}{\partial \mathbf{x}}(\mathbf{x}) + \mathbf{g}u, \tag{14}$$

where $\mathbf{R} = \mathbf{R}^T \geqslant 0$, $\mathbf{J} = -\mathbf{J}^T$, and $\mathbf{g}$ are the damping, interconnection and input matrices respectively, and they are given by,

$$\mathbf{R} = \begin{bmatrix} 0 & 0 & 0 \\ 0 & b_2 & 0 \\ 0 & 0 & \frac{b_3}{b_1} \end{bmatrix}, \quad \mathbf{J} = \begin{bmatrix} 0 & 1 & 0 \\ -1 & 0 & 0 \\ 0 & 0 & 0 \end{bmatrix}, \quad \mathbf{g} = \begin{bmatrix} 0 \\ 0 \\ 1 \end{bmatrix}. \tag{15}$$

3. Control strategies

The different nonlinear and linear control strategies will be described in this section. For a better understanding of the strategy design, a brief description of each methodology is first introduced in each subsection, and then, based on it, there is a description of its application to the synchronous generator.

3.1. Control via feedback linearization

3.1.1. Design methodology

The purpose of feedback linearization (FL) is to cancel nonlinearities and to impose a linear dynamics. With this aim, the state transformation $\mathbf{z} = \mathbf{T}(\mathbf{x})$ and the input transformation $u = u(\mathbf{x}, v)$ are found first. By applying these transformations, the nonlinear dynamics $\dot{\mathbf{x}} = \mathbf{f}(\mathbf{x}) + \mathbf{g}(\mathbf{x})u$ becomes a linear time-invariant (LTI) dynamics equivalent ($\dot{\mathbf{z}} = \mathbf{A}\mathbf{z} + \mathbf{b}v$). Then, linear control techniques are used to design the auxiliary control input v.

The procedure consists of calculating the linearizing function (named $\lambda(\mathbf{x})$ in this paper) at first. Such function is obtained by solving the following partial differential equation (PDE) system,[1]

$$\begin{bmatrix} ad_{\mathbf{f}}^0 \mathbf{g} & ad_{\mathbf{f}}^1 \mathbf{g} & \dots & ad_{\mathbf{f}}^{n-2} \mathbf{g} & ad_{\mathbf{f}}^{n-1} \mathbf{g} \end{bmatrix} \begin{bmatrix} \frac{\partial \lambda}{\partial x_1} \\ \frac{\partial \lambda}{\partial x_2} \\ \vdots \\ \frac{\partial \lambda}{\partial x_{n-1}} \\ \frac{\partial \lambda}{\partial x_n} \end{bmatrix} = \begin{bmatrix} 0 \\ 0 \\ \vdots \\ 0 \\ 1 \end{bmatrix}. \tag{16}$$

Once obtained the linearizing function, when there is one, it is possible to calculate the state transformation as,[2]

$$\mathbf{z} = \mathbf{T}(\mathbf{x}) = \begin{bmatrix} \lambda & L_{\mathbf{f}}\lambda \dots L_{\mathbf{f}}^{n-1}\lambda \end{bmatrix}^T. \tag{17}$$

Consequently, taking the time derivative of (17), it is obtained

$$\dot{\mathbf{z}} = \frac{\partial \mathbf{T}}{\partial \mathbf{x}} \dot{\mathbf{x}}. \tag{18}$$

The control law which linearizes the system is given by (see Ref. [44] for a deeper description),

$$u = \frac{-L_{\mathbf{f}}^n \lambda}{L_{\mathbf{g}} L_{\mathbf{f}}^{n-1} \lambda} + \frac{1}{L_{\mathbf{g}} L_{\mathbf{f}}^{n-1} \lambda} v. \tag{19}$$

Finally, using the expressions (17) and (18), the system given in the original coordinates by,

$$\dot{\mathbf{x}} = \mathbf{f}(\mathbf{x}) + \mathbf{g}(\mathbf{x})u, \tag{20}$$

is represented in the transformed domain as,

$$\frac{\partial \mathbf{T}^{-1}}{\partial \mathbf{x}} \dot{\mathbf{z}} = \mathbf{f}(\mathbf{T}^{-1}(\mathbf{z})) + \mathbf{g}(\mathbf{T}^{-1}(\mathbf{z}))u, \tag{21}$$

then,

$$\dot{\mathbf{z}} = \frac{\partial \mathbf{T}}{\partial \mathbf{x}} \mathbf{f}(\mathbf{T}^{-1}(\mathbf{z})) + \frac{\partial \mathbf{T}}{\partial \mathbf{x}} \mathbf{g}(\mathbf{T}^{-1}(\mathbf{z}))u = \mathbf{m}(\mathbf{z}) + \mathbf{n}(\mathbf{z})u. \tag{22}$$

By using (19) in (22), the following system description results:

$$\dot{\mathbf{z}} = \mathbf{A}\mathbf{z} + \mathbf{b}v. \tag{23}$$

Now, linear strategies such as linear quadratic regulation, pole assignment, tracking error dynamics, etc. could be used for controlling the linear system (23) represented in the new coordinates $\mathbf{z}$.

[1] The simplified notation within Lie brackets $ad_{\mathbf{f}}^i \mathbf{g} = \left[\mathbf{f}, ad_{\mathbf{f}}^{i-1} \mathbf{g}\right]$, with $ad_{\mathbf{f}}^0 \mathbf{g} = \mathbf{g}$, and $i = 1,2,\dots$ has been used (see Ref. [44] for further details).

[2] Where $L_{\mathbf{f}}^{n-1}\lambda$ is the λ Lie derivative of $(n-1)$ order with respect to $\mathbf{f}$, being n the system order.

3.1.2. Feedback linearization applied to the synchronous generator

First, the linearizing function is calculated by applying the expression (16), and by using $\mathbf{f}(\mathbf{x})$ and $\mathbf{g}$ defined in (5) and (6). In this way the following PDE system is obtained,

$$
\begin{aligned}
&-b_1 \sin x_1 \frac{\partial \lambda}{\partial x_3} = 0,\\
&\sin x_1 \frac{\partial \lambda}{\partial x_2} + (x_2 \cos x_1 + (b_2 + b_4)\sin x_1)\frac{\partial \lambda}{\partial x_3} = 0,\\
&\frac{\partial \lambda}{\partial x_1} + b_4 \frac{\partial \lambda}{\partial x_2} + b_4^2 \frac{\partial \lambda}{\partial x_3} = 1.
\end{aligned}
$$

The solution to the previous system is $\lambda(\mathbf{x}) = x_1 + \mathbb{C}$. By choosing the simplest arbitrary solution one gets $\lambda(\mathbf{x}) = x_1$. The system transformation calculated from (17) results,

$$
\mathbf{T}(\mathbf{x}) = \begin{bmatrix} z_1 \\ z_2 \\ z_3 \end{bmatrix} = \begin{bmatrix} x_1 \\ x_2 \\ -b_1 x_3 \sin x_1 - b_2 x_2 + P \end{bmatrix}. \tag{24}
$$

The inverse transformation is given by,

$$
\mathbf{T}^{-1}(\mathbf{z}) = \begin{bmatrix} x_1 \\ x_2 \\ x_3 \end{bmatrix} = \begin{bmatrix} z_1 \\ z_2 \frac{1}{b_1}(P - b_2 z_2 - z_3)\csc z_1 \end{bmatrix}. \tag{25}
$$

Then, the control law is determined by the Eq. (19),

$$
\begin{aligned}
u = -(b_1 \sin x_1)^{-1}[v + b_2(P - b_2 x_2) + b_1 x_2 x_3 \cos x_1 + b_1(E\\
- (b_2 + b_4)x_3 + b_3 \cos x_1)\sin x_1].
\end{aligned} \tag{26}
$$

The following linearized system is obtained by using (26):

$$
\begin{bmatrix} \dot{z}_1 \\ \dot{z}_2 \\ \dot{z}_3 \end{bmatrix} = \begin{bmatrix} 0 & 1 & 0 \\ 0 & 0 & 1 \\ 0 & 0 & 0 \end{bmatrix} \begin{bmatrix} z_1 \\ z_2 \\ z_3 \end{bmatrix} + \begin{bmatrix} 0 \\ 0 \\ 1 \end{bmatrix} v. \tag{27}
$$

Finally, it only remains to design the auxiliary control input v, from the linear system (27) using any classical linear control technique.

3.2. Control via L_gV

3.2.1. Design methodology

First, we consider nonlinear systems like $\dot{\mathbf{x}} = \mathbf{f}(\mathbf{x}) + \mathbf{g}(\mathbf{x})\mathbf{u}$, with stable equilibrium point in $\mathbf{x}^\star$ for an open-loop system $\dot{\mathbf{x}} = \mathbf{f}(\mathbf{x})$. Therefore, there exists a Lyapunov function, $V(\mathbf{x})$, which satisfies [44],

$$
\begin{aligned}
&V(\mathbf{x}^\star) = 0,\\
&V(\mathbf{x}) > 0, \quad \forall\, \mathbf{x} \in \{D - \mathbf{x}^\star\},\\
&\dot{V}(\mathbf{x}) = \tfrac{\partial V(\mathbf{x})}{\partial \mathbf{x}}\dot{\mathbf{x}} = \tfrac{\partial V(\mathbf{x})}{\partial \mathbf{x}}\mathbf{f}(\mathbf{x}) = L_{\mathbf{f}}V \leqslant 0.
\end{aligned} \tag{28}
$$

The $V(\mathbf{x})$ time derivative, calculated on the closed-loop system, results

$$
\begin{aligned}
\dot{V}(\mathbf{x}) &= \frac{\partial V(\mathbf{x})}{\partial \mathbf{x}}\dot{\mathbf{x}} = \frac{\partial V(\mathbf{x})}{\partial \mathbf{x}}(\mathbf{f}(\mathbf{x}) + \mathbf{g}(\mathbf{x})\mathbf{u}),\\
&= L_{\mathbf{f}}V + L_{\mathbf{g}}V\mathbf{u}.
\end{aligned} \tag{29}
$$

Considering the following control law [33],

$$
\mathbf{u} = -k_v(L_{\mathbf{g}}V)^T, \quad k_v > 0 \tag{30}
$$

and replacing (30) in (29) results,

$$
\begin{aligned}
\dot{V}(\mathbf{x}) &= L_{\mathbf{f}}V + L_{\mathbf{g}}V\mathbf{u},\\
&= L_{\mathbf{f}}V - \underbrace{L_{\mathbf{g}}Vk_v(L_{\mathbf{g}}V)^T}_{>0} \leqslant L_{\mathbf{f}}V \leqslant 0.
\end{aligned} \tag{31}
$$

Therefore, with the control law (30) (which is the reason of the technique name), closed-loop stability and an enhancement in system damping for being $\dot{V}_{closed-loop} \leqslant \dot{V}_{open-loop}$ are attained. The L_gV control is always stable, no matter how high the k_v value is chosen (infinite gain margin). Besides, this strategy has the quality of not changing the equilibrium point of the open-loop system (that is, $\mathbf{u}|_{\mathbf{x}^\star} = 0$).

3.2.2. L_gV Control applied to the synchronous generator

As $V(\mathbf{x})$ Lyapunov function the expression (13) will be used, then $V(\mathbf{x}) = H(\mathbf{x})$. An L_gV controller for the system (4), satisfying (28), could be directly determined by applying the Eq. (30). It results in the following control law:

$$
\begin{aligned}
u &= -k_v \frac{\partial V(\mathbf{x})}{\partial \mathbf{x}}\mathbf{g} = -k_v \frac{\partial V(\mathbf{x})}{\partial x_3},\\
&= -k_v\left(b_1(\cos x_1^\star - \cos x_1) + \frac{b_1 b_4}{b_3}(x_3 - x_3^\star)\right).
\end{aligned} \tag{32}
$$

3.3. Control via interconnection and damping assignment (IDA)

3.3.1. Design methodology

In order to shape the system energy by changing its interconnection and damping, a dynamic model representation including these features must be formulated. The PCH representation (14) is considered for this purpose (for a further detailed development of this strategy see [45]),

$$
\dot{\mathbf{x}} = [\mathbf{J}(\mathbf{x}) - \mathbf{R}(\mathbf{x})]\frac{\partial H}{\partial \mathbf{x}}(\mathbf{x}) + \mathbf{g}(\mathbf{x})\mathbf{u}, \tag{33}
$$

$$
\mathbf{y} = \mathbf{g}^T(\mathbf{x})\frac{\partial H}{\partial \mathbf{x}}(\mathbf{x}), \tag{34}
$$

where $H(\mathbf{x})$ is the system energy function, $\mathbf{J}(\mathbf{x}) = -\mathbf{J}^T(\mathbf{x})$ contains the interconnecting internal structure and $\mathbf{R}(\mathbf{x}) = \mathbf{R}^T(\mathbf{x}) \geqslant 0$ is the damping matrix. The technique selects the interconnection and damping structures so that the controller achieves the following closed-loop dynamics,

$$
\dot{\mathbf{x}} = [\mathbf{J}_d(\mathbf{x}) - \mathbf{R}_d(\mathbf{x})]\frac{\partial H_d}{\partial \mathbf{x}}(\mathbf{x}), \tag{35}
$$

where $H_d(\mathbf{x})$ is the desired energy function and has a local minimum at the desired $\mathbf{x}^\star$ operation point, while $\mathbf{J_d}(\mathbf{x}) = -\mathbf{J_d}^T(\mathbf{x})$ and $\mathbf{R_d}(\mathbf{x}) = \mathbf{R_d}^T(\mathbf{x}) \geqslant 0$ are the new desired interconnection and damping matrices. Matrices to be used later are defined as,

$$
\mathbf{J}_a(\mathbf{x}) \triangleq \mathbf{J}_d(\mathbf{x}) - \mathbf{J}(\mathbf{x}), \tag{36}
$$

$$
\mathbf{R}_a(\mathbf{x}) \triangleq \mathbf{R}_d(\mathbf{x}) - \mathbf{R}(\mathbf{x}), \tag{37}
$$

$$
H_a(\mathbf{x}) \triangleq H_d(\mathbf{x}) - H(\mathbf{x}). \tag{38}
$$

Next, to simplify notation, the state dependence will be omitted. Equaling (33) and (35) and considering (36)–(38) results,

$$
\begin{aligned}
[\mathbf{J} - \mathbf{R}]\frac{\partial H}{\partial \mathbf{x}} + \mathbf{g}\mathbf{u} &= [\mathbf{J}_d - \mathbf{R}_d]\frac{\partial H_d}{\partial \mathbf{x}},\\
&= [\mathbf{J} - \mathbf{R}]\frac{\partial H}{\partial \mathbf{x}}(\mathbf{x}) + [\mathbf{J}_a - \mathbf{R}_a]\frac{\partial H}{\partial \mathbf{x}} + [\mathbf{J}_d - \mathbf{R}_d]\frac{\partial H_a}{\partial \mathbf{x}},
\end{aligned}
$$

then,

$$
[\mathbf{J}_d - \mathbf{R}_d]\frac{\partial H_a}{\partial \mathbf{x}} + [\mathbf{J}_a - \mathbf{R}_a]\frac{\partial H}{\partial \mathbf{x}} - \mathbf{g}\mathbf{u} = \mathbf{0}. \tag{39}
$$

Eq. (39) represents a PDE system which needs to be solved to obtain the energy function assigned H_a. Such function must be particularized to satisfy certain requisites so that the H_d closed-loop energy function presents a minimum at the desired $\mathbf{x}^\star$ operation point. In order for H_d to have a stable equilibrium point in $\mathbf{x}^\star$ the following conditions should be satisfied,

$$\left.\frac{\partial H_d}{\partial \mathbf{x}}\right|_{\mathbf{x}^\star} = 0, \tag{40}$$

$$\left.\frac{\partial H_d^2}{\partial \mathbf{x}^2}\right|_{\mathbf{x}^\star} > 0, \tag{41}$$

or in a similar way, considering (36)–(38),

$$\left.\frac{\partial H_a}{\partial \mathbf{x}}\right|_{\mathbf{x}^\star} = -\left.\frac{\partial H}{\partial \mathbf{x}}\right|_{\mathbf{x}^\star}, \tag{42}$$

$$\left.\frac{\partial H_a^2}{\partial \mathbf{x}^2}\right|_{\mathbf{x}^\star} > -\left.\frac{\partial H^2}{\partial \mathbf{x}^2}\right|_{\mathbf{x}^\star}. \tag{43}$$

Finally, the controller can be calculated from (39), yielding

$$\mathbf{u} = (\mathbf{g}^T\mathbf{g})^{-1}\mathbf{g}^T\left([\mathbf{J}_d - \mathbf{R}_d]\frac{\partial H_a}{\partial \mathbf{x}} + [\mathbf{J}_a - \mathbf{R}_a]\frac{\partial H}{\partial \mathbf{x}}\right). \tag{44}$$

When from (39), it is possible to obtain a H_a function verifying conditions (42), (43), then a closed-loop system (35) with controller given by (44) is obtained. Besides, $\mathbf{x}^\star$ will be a locally stable equilibrium point, where the asymptotic stability of $\mathbf{x}^\star$ can be evaluated through La Salle's theorem [44].

3.3.2. IDA applied to the synchronous generator

The desired closed-loop interconnection and damping matrices will be chosen as (see [34]),

$$\mathbf{J}_d = \begin{bmatrix} 0 & 1 & 0 \\ -1 & 0 & \alpha_1 \\ 0 & -\alpha_1 & 0 \end{bmatrix}, \quad \mathbf{R}_d = \begin{bmatrix} 0 & 0 & 0 \\ 0 & b_2 & 0 \\ 0 & 0 & \frac{b_3}{b_1} + k_v \end{bmatrix}. \tag{45}$$

The term $k_v \geqslant 0$ is inserted to improve the energy dissipation in the electric variable, as it is done by L_gV controllers. At the same time, the α_1 coefficients are added to the interconnection matrix because the open-loop system does not present a direct coupling between electric and mechanical dynamics. With closed-loop matrices already defined, the PDE system of Eq. (39) is solved, and using the definitions (36)–(38), the following equations result:

$$0 = \frac{\partial H_a}{\partial x_2}, \tag{46}$$

$$0 = b_1\alpha_1\left(\frac{b_4}{b_3}(x_3 - x_3^\star) - \cos x_1 + \cos x_{1*}\right) + \alpha_1\frac{\partial H_a}{\partial x_3} - b_2\frac{\partial H_a}{\partial x_2} - \frac{\partial H_a}{\partial x_1}, \tag{47}$$

$$0 = u + \alpha_1 x_2 - b_1 k_v\left(\frac{b_4}{b_3}(x_3^\star - x_3) + \cos x_1 - \cos x_1^\star\right) + \left(\frac{b_3}{b_1} + k_v\right)\frac{\partial H_a}{\partial x_3} + \alpha_1\frac{\partial H_a}{\partial x_2}. \tag{48}$$

The controller is calculated by using Eq. (48). Then, it only remains to determine H_a which is obtained by solving the system (46), (47) yielding,

$$H_a(\mathbf{x}) = b_1\alpha_1\left(\frac{b_4 x_1}{b_3}\left(\frac{\alpha_1 x_1}{2} + (x_3 - x_3^\star)\right) + x_1\cos x_1^\star - \sin x_1\right) + \Phi[\alpha_1 x_1 + x_3], \tag{49}$$

where Φ is an arbitrary function. This function will be chosen to verify (42). The following restriction over Φ is obtained when evaluating the mentioned condition,

$$\dot{\Phi}[\alpha_1 x_1^\star + x_3^\star] = -\frac{b_1 b_4}{b_3}\alpha_1 x_1^\star \triangleq \beta_1. \tag{50}$$

A quadratic function on the error of $[\alpha_1 x_1 + x_3]$ is arbitrarily proposed for Φ to fulfill with (50). Therefore,

$$\Phi[\alpha_1 x_1 + x_3] \triangleq \beta_1(\alpha_1(x_1 - x_1^\star) + (x_3 - x_3^\star)) + \beta_2(\alpha_1(x_1 - x_1^\star) + (x_3 - x_3^\star))^2. \tag{51}$$

The gain stability boundaries are obtained from the condition (41) which implies the Hessian calculation of H_d,

$$\left.\frac{\partial H_d^2}{\partial \mathbf{x}^2}\right|_{\mathbf{x}^\star} = \begin{bmatrix} \gamma + b_1 x_3^\star\cos x_1^\star + b_1\alpha_1\left(\frac{b_4\alpha_1}{b_3} + \sin x_1^\star\right) & 0 & \frac{\gamma}{\alpha_1} + \frac{b_1 b_4\alpha_1}{b_3} + b_1\sin x_1^\star \\ 0 & 1 & 0 \\ \frac{\gamma}{\alpha_1} + \frac{b_1 b_4\alpha_1}{b_3} + b_1\sin x_1^\star & 0 & \alpha_2 \end{bmatrix}$$

which will be defined as a positive-definite matrix, if it fulfills the following conditions:

$$\alpha_2 \geqslant \frac{b_1 b_4}{b_3}, \quad \alpha_1 < -\frac{b_1}{\alpha_2}, \tag{52}$$

where $\alpha_2 \triangleq \frac{b_1 b_4}{b_3} + \frac{\gamma}{\alpha_1^2}$, and $\gamma \triangleq 2\alpha_1^2\beta_2$ have been defined. Then, the controller u governing the generator field voltage is obtained from (48), and (49), (51) expressions are used for H_a, where gains must verify conditions (52) to ensure stability. In this way, the control signal is calculated as,

$$u = -k_v b_1(\cos x_1^\star - \cos x_1) - \alpha_1\alpha_2\left(\frac{b_3}{b_1} + k_v\right)(x_1 - x_1^\star) - \alpha_1 x_2 - \left(\frac{b_3}{b_1}\alpha_2 - b_4 + k_v\alpha_2\right)(x_3 - x_3^\star). \tag{53}$$

3.4. PSS controller

The PSS is a controller based on transfer functions and currently used in big generators. It is placed with the aim of damping rotor oscillations via an auxiliary signal in the excitation system. It can include a component in the electric torque generated by the machine which, by being in phase with the speed variation, can reduce the angle oscillation. In Fig. 2 an outline of the AVR-PSS configuration type IEEE ST1A-PSS1A is shown and used for the comparison. In this way, nonlinear control strategies are not only compared among them but also with a conventional PSS scheme.

The PSS consists of a K_S gain which is used to determine the amount of damping to be injected. Then, a washout filter makes it just act against oscillations in the input signal (transient state) to avoid steady-state error in the terminal voltage. In addition, a series of lead-phase filters are also included (phase compensation stage) to eliminate any delay between the excitation and the electric torque. In this way, the signal can arrive with the correct phase to counteract oscillations.

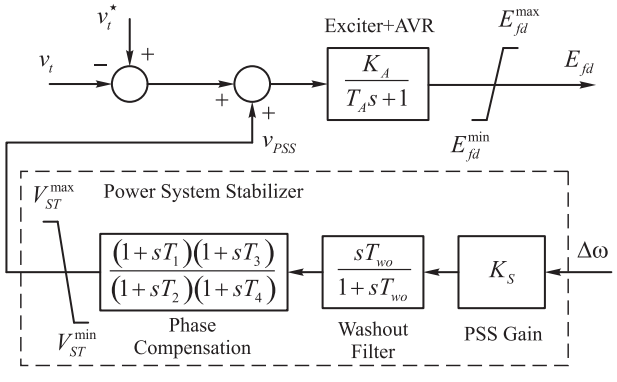

Fig. 2. Block diagram of AVR plus PSS.

4. Generator terminal voltage regulation

An important specification to be satisfied by the controller is to increase the angle transient stability. However, it is also needed that the same controller presents a good terminal post-fault voltage regulation. Nevertheless, the generator terminal voltage v_t does not appear in an explicit way when a nonlinear controller is designed based on the original states $\mathbf{x}$ ($x_1 = \delta,\ x_2 = \Delta\omega,\ x_3 = E'_q$) or the transformed states $\mathbf{z}$ ($z_1 = \delta$, $z_2 = \Delta\omega$, $z_3 = \alpha$ (rotor acceleration)). Generally, network topology changes when a fault occurs; thus, in order to keep the terminal voltage value, a new load angle must be calculated. However, the knowledge of the post-fault load angle is possible when full information of the network is available requiring a power flow computation. This option is not viable from the controller implementation point of view. On the other hand, if the value of the pre-fault load angle is maintained then, the voltage will reach an abnormal value when the network topology is modified [32,46]. In order to deal with this problem some solutions can be found in the literature. In what follows, these solutions are briefly developed.

4.1. Switched control law

When a switched control law is used, the load angle is controlled immediately after the fault occurrence. Then, after a fixed period of time the controller is switched to a voltage regulation mode. This procedure is described in [47,29,38,48]. For example, in references [47,29,48] a feedback linearization controller is built with transformed states $\mathbf{z} = [\delta\ \omega\ \Delta P_e]^T$, where ΔP_e is the variation of the generator electric power. In this FL control the auxiliary control input v has the following two expressions:

$$v_1 = -k_\delta\delta - k_\omega\omega - k_P\Delta P_e \quad t_0 \leqslant t < t_1 \tag{54}$$

$$v_2 = -k_v\Delta v_t - k_\omega\omega - k_P\Delta P_e \quad t_1 \leqslant t \tag{55}$$

where Δv_t is the terminal voltage deviation. The first expression v_1 controls the load angle (transient stability), and the second one v_2 allows to regulate the generator terminal voltage at the post-fault period, whereas t_0 and t_1 are the commutation times. Nevertheless, commutation times must be established based on a previous knowledge of the kind of fault and then the method lacks of robustness. An improved technique has been proposed in [32], where the commutation law is based on smooth transitions. Soft commutations are accomplished using membership functions μ, and the auxiliary control input v is obtained as,

$$v = \mu_\delta v_1 + \mu_v v_2. \tag{56}$$

However, the proper membership functions are hard to find, and must be designed by trial-and-error procedures in digital simulations.

4.2. Dynamic term approach

In [49] an additional term, from an AVR-like structure, is included to the auxiliary control variable v. This term ($K_{va}v_a$) achieves the post-fault voltage regulation, when changes in the operating conditions or network topology occur. In this way, the drawback that the terminal voltage is not present in the original nonlinear controller design is overcome. Using the Eq. (27) and considering the physical significance of the transformed states $\mathbf{z}$, this approach results in,

$$\dot{\delta} = \Delta\omega \tag{57}$$

$$\Delta\dot{\omega} = \alpha \tag{58}$$

$$\dot{\alpha} = v - K_{va}v_a \tag{59}$$

$$T_a\dot{v}_a = -v_a + K_a(v^\star - v_t). \tag{60}$$

Unfortunately, this proposal reintroduces nonlinearities to the system, because terminal voltage and states are nonlinearly related. Moreover, the term $K_{va}v_a$ should only act in the post-transient period for recovering the terminal voltage. Therefore, it must be tuned to be smaller than v in order to maintain the linear dynamics given by the feedback linearization controller. Consequently, K_{va}, T_a and K_a setting should be carefully made.

4.3. Additional AVR

Similarly to the above-mentioned technique, in [50–52] a term provided by a conventional AVR is added to the field voltage obtained from the load angle controller. Nevertheless, the load angle controller design does not consider the AVR dynamics. Consequently, the additional AVR term must be also carefully tuned to avoid interactions with the main controller.

4.4. Static reference of the load angle

When there are changes in the network topology, it is possible to recover the pre-fault value of the terminal voltage while a load angle controller is used. It is achieved by calculating the new angle δ for a desired terminal voltage. Strategies pursuing this idea can be found in [53] (scheme called observation decoupled state space) and in the improved versions [54–57]. By using a similar procedure to that described in [57], it is possible to obtain the following expression which relates the desired terminal voltage $v_t^\star$ with the load angle reference $\delta^\star$,

$$v_t^{\star 2} = \left(\frac{X_q v_r}{X_q + X_r}\right)^2 + \left(\frac{X_r P_m \csc\delta^\star}{v_r}\right)^2 + \frac{2X_qX_rP_m\cot\delta^\star}{X_q + X_r} \tag{61}$$

where the steady-state synchronous generator equations were used, and resistance losses have been neglected. In Eq. (61) v_r and X_r stand for the high-side transformer voltage and reactance, respectively. From (61) the load angle reference is obtained for a certain voltage v_r and mechanical power P_m, when a terminal voltage $v_t^\star$ is desired. Then, the angle $\delta^\star$is given as a reference to the nonlinear load angle controller. Note that the Eq. (61) is transcendental, so numerical methods must be employed for solving it.

This technique does not reintroduce nonlinearities to the system, and does not need any parameter tuning. In this way, the linear characteristic of the transformed system is maintained. However, it must be noted that in the load angle reference calculation (61), the voltage v_r is needed. Therefore, when this technique is used in a weak multimachine system, after big disturbances, v_r voltage presents oscillations that are propagated to the load angle

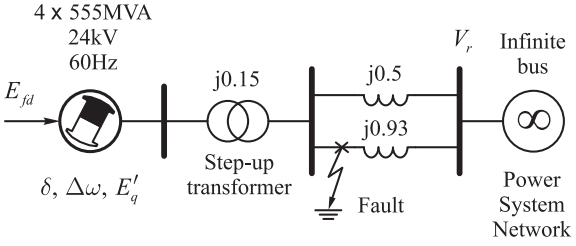

Fig. 3. Schematic of the single-machine test system.

Table 2
Critical fault-clearing time (ms).

Controller	Open-loop	FL	IDA	PSS
t_{cr}	54	108	104	107

reference. This situation could deteriorate the angle damping. In order to overcome this drawback, and considering that we do not intend to recover the terminal voltage immediately after the disturbance, a low-pass filter is placed in the output of the angle reference calculation. Consequently, the voltage oscillations are blocked and do not diminish the controller performance. Then, the terminal voltage is slowly recovered after the disturbance transient. The low-pass filter design is easier than the three-parameter tuning (K_{va}, K_a, T_a) proposed in the dynamic term approach.

4.5. Dynamic reference of the load angle

In order to overcome the drawbacks introduced by the above approaches, an alternative strategy can be considered. This technique combines presented solutions obtaining the load angle reference from a dynamic term given by a PI regulator,

$$\delta^{\star} = K_{Pvt}\left(v_t - v_t^{\star}\right) + K_{Ivt}\int \left(v_t - v_t^{\star}\right)dt. \tag{62}$$

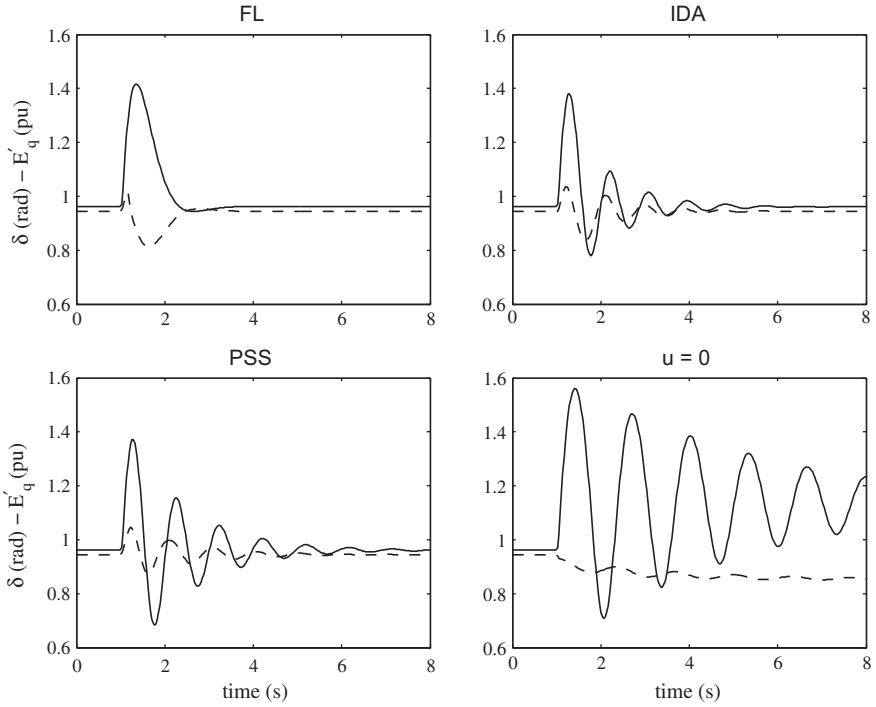

Fig. 4. Load angle (solid) and transient EMF (dashed), t_{fc} = 54 ms.

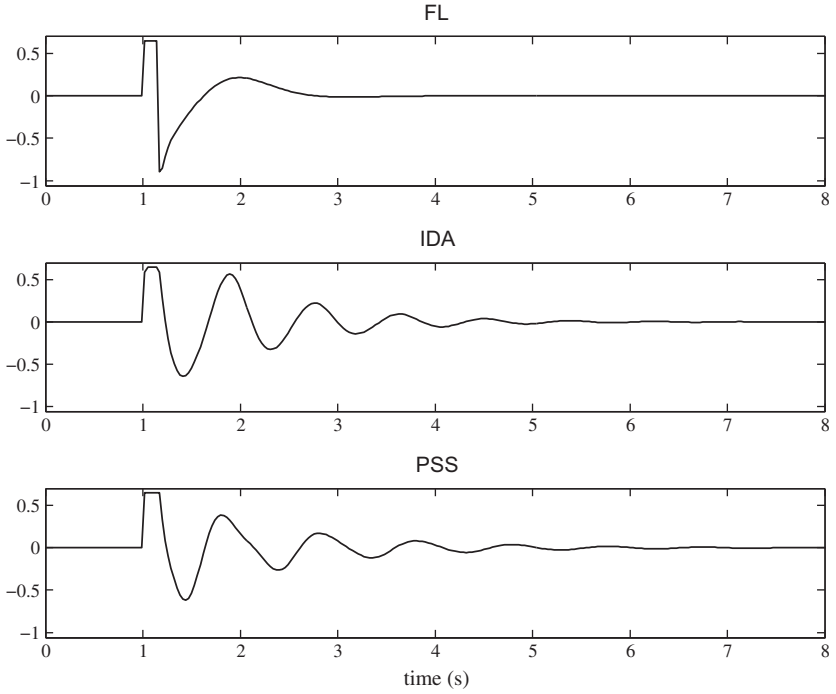

Fig. 5. Controller action u, with t_{fc} = 54 ms.

This term, as in the above cases, must be tuned for moving $\delta^{\star}$ slowly. In this way, there is not interaction with the main nonlinear control (for example, keeping the linear characteristic given by the FL controller) and the desired terminal voltage value is recovered in the post-fault period. The voltage regulation based on the dynamic reference is an outer control loop and the load angle controller is an inner control loop, as in a cascade control approach. Therefore, by setting the bandwidth of the outer loop slower than the inner loop any interaction between them is prevented.

To conclude this section, it must be noted that some authors (for instance in [49,30,58,55,59]) prefer to consider the generator terminal voltage as an output to be linearized in the FL technique. Thus, the voltage is rapidly regulated, but the angle stability is deteriorated. From our researches and tests, we infer that the option of using a δ angle controller along with the dynamic reference technique is better when transient stability must be increased and the terminal voltage must be regulated in a post-transient period.

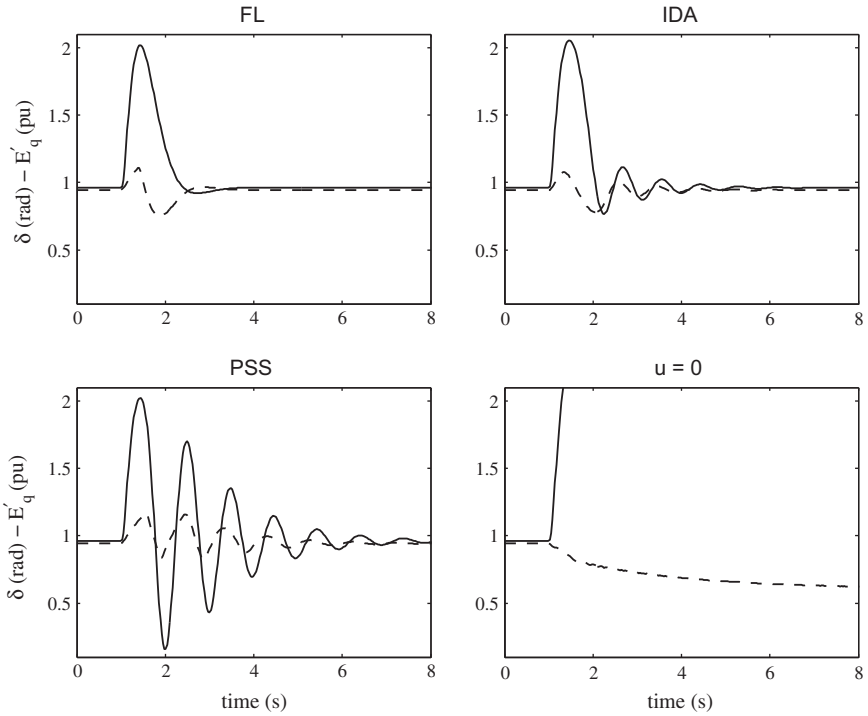

Fig. 6. Load angle (solid) and transient EMF (dashed), t_{fc} = 100 ms.

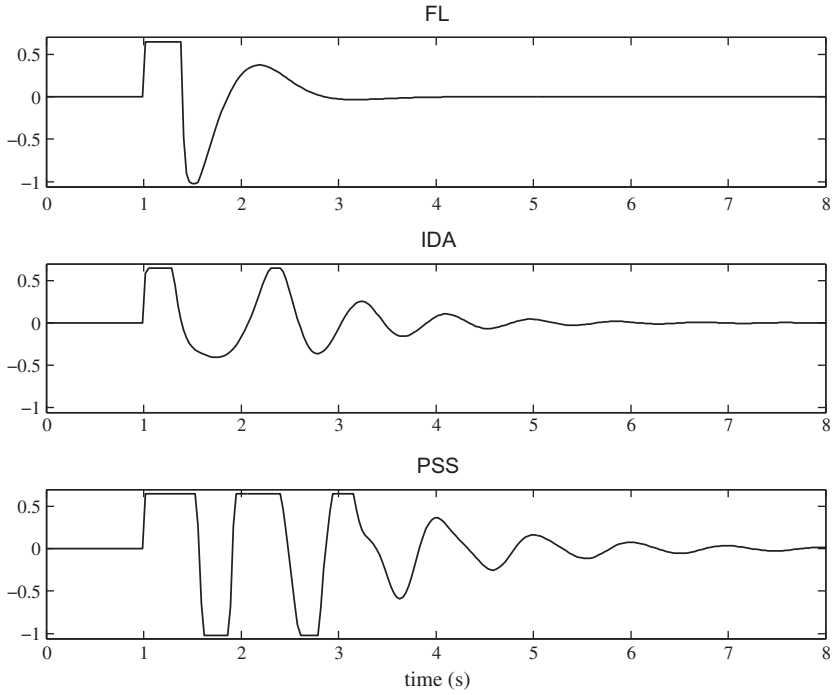

Fig. 7. Controller action u, with t_{fc} = 100 ms.

For this reason, this latter approach is implemented in the performance assessment section.

5. Performance assessment

Two examples are chosen to compare the performance and robustness of the different control strategies. First, we consider a single-machine test from example 13.2 of [42] and then, a two-area four-machine test from example 12.6 of [42]. Excitation systems are the IEEE-ST1A based on static elements with a fast dynamic response. To compare the nonlinear strategies with current solutions, we consider the power system stabilizer IEEE-PSS1A, the parameters of which have also been extracted from the mentioned examples (see its configuration in Fig. 2). The power system and control strategies have been implemented by using the SimPowerSystems blockset of MATLAB®.

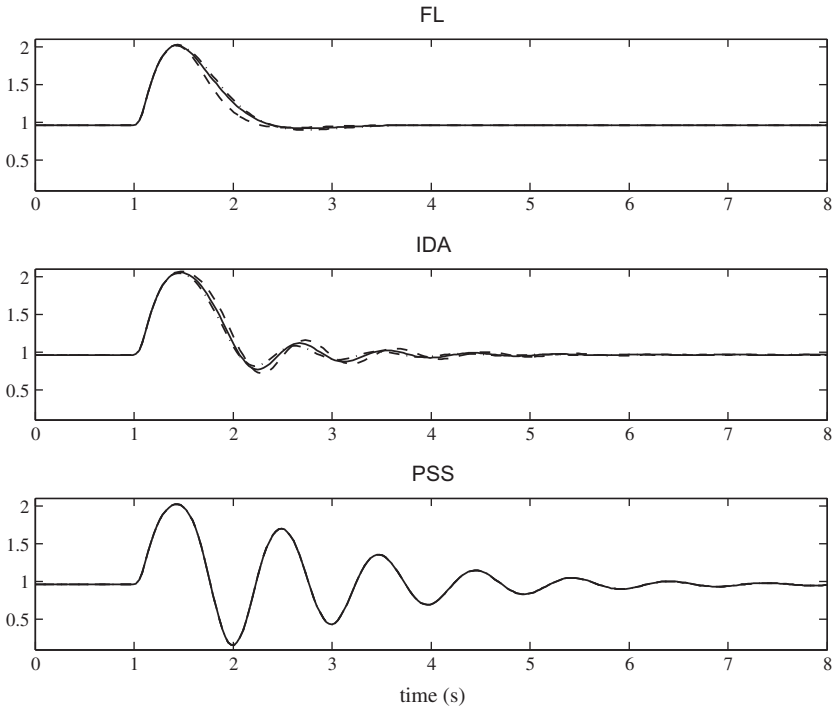

Fig. 8. Sensitivity of the load angle δ to the voltage variation at the infinite bus. $\Delta V_r = -15\%$ (dashed), $\Delta V_r = 15\%$ (dot-line).

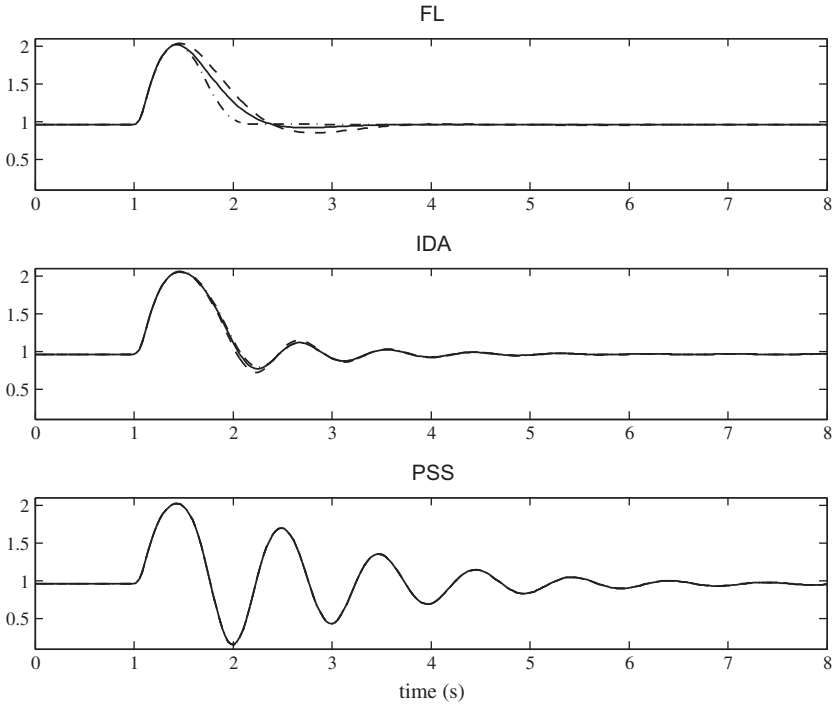

Fig. 9. Sensitivity of the load angle δ to the variation in the external reactance. $\Delta X_E = -50\%$ (dashed), $\Delta X_E = 50\%$ (dot-line).

In order to study the behavior of each control strategy, great disturbances (short circuits) and parametric uncertainties have been performed. Tuning of control strategies is done so that each one has the best possible performance. The FL linear loop has been tuned using linear quadratic optimal control. IDA has been tuned so that the design parameters verify the stability condition (52) in the same way as it is designed in [34]. AVR-PSS parameters are taken from examples 13.2 and 12.6 of reference [42]. For space and clarity reasons, graphics corresponding to L_gV control are not included. However, as it was mentioned, L_gV control is a particular case of IDA control, therefore without loss of generality, this will not be plotted in the below graphics.

5.1. Single-machine test

The system used in this section is a single-machine test from example 13.2 of [42], and it is illustrated in Fig. 3. It consists of a synchronous generator, with its step-up transformer, connected via two lines in parallel to a big power system network, which will be modeled like an infinite bus. System data and control design parameters of both PSS and nonlinear controllers are given in Table 1.

5.1.1. Transient performance

Transient performance is assessed by provoking a three-phase fault in terminals on the high-voltage side of the transformer, as it is seen in Fig. 3. Two main features for each controller are analyzed. One of them is the maximum short-circuit time for which the synchronism is maintained (critical fault-clearing time, t_{cr}), and the other one is the load angle oscillation damping after the fault is produced.

Critical time for open and closed loops are shown in Table 2. It must be remarked that the critical time of the controlled case duplicates the critical time of the uncontrolled case. However, there are not significant differences among controllers in this issue.

In order to assess the damping injected to the system using each strategy, two cases are analyzed: one for a 54 ms fault time (t_{fc}) and another, and more demanding one, for a 100 ms fault. The load angle δ and transient EMF E'_q for the first study case are shown in Fig. 4. It can be seen there that the system without controller does

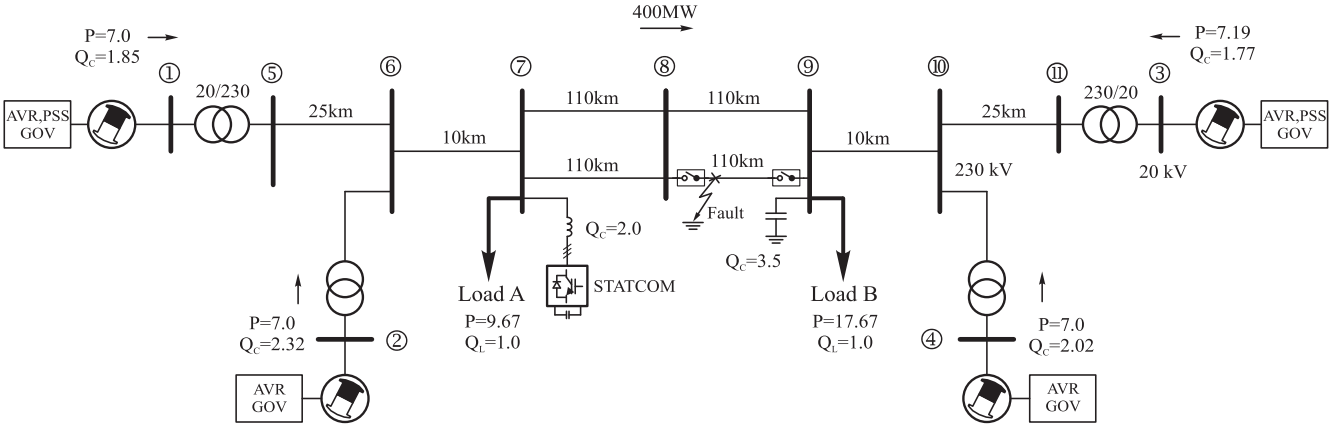

Fig. 10. Single-line diagram of the two-area four-machine test system.

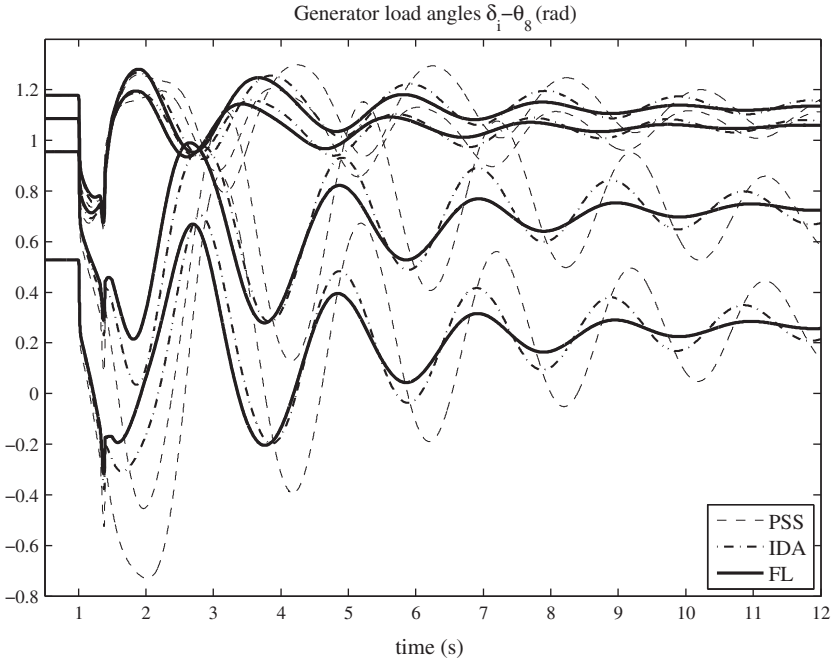

Fig. 11. Load angles of each generator for PSS, IDA and FL controllers.

not lose synchronism. Thus, it is possible to compare the damping injection for each controller in relation to the uncontrolled case. The best dynamic behavior regarding the damping injection is presented by FL. When IDA and PSS are used, a small oscillation is kept. Fig. 5 shows the control signals (field voltage variation) of the tested controllers. It is noticeable that the control effort and the energy used by FL is lower than PSS and IDA energies.

Figs. 6 and 7 show the same states for a more severe short circuit of 100 ms. Note that, in this case, the open-loop system becomes unstable. Roughly speaking, similar conclusions to the first study case of $t_{fc} = 54$ ms are obtained with respect to the system behavior. Nevertheless, IDA has a better performance than PSS because this more severe disturbance makes states to go beyond the operation point in which PSS is tuned. From the performance point of view, it is clear that better results are attained when nonlinear control strategies are used.

5.1.2. Robustness against parameter uncertainties

Sensitivity of strategies to parameter uncertainties is shown in Figs. 8 and 9, where the V_r infinite bus voltage and the X_E external reactance have been chosen as uncertain values due to their greater variation in power system work conditions. It can be concluded

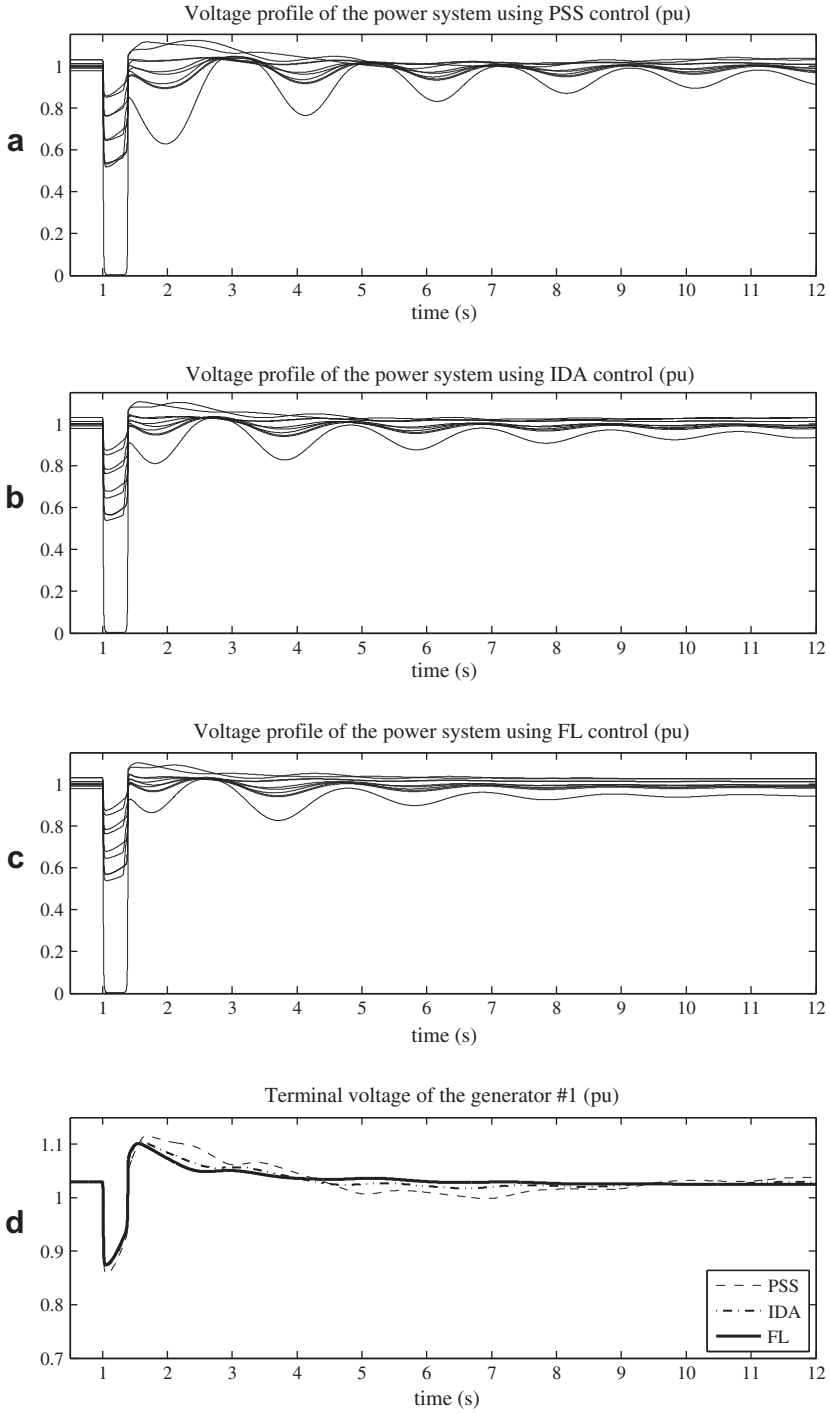

Fig. 12. Voltage profiles of the power system using the different control strategies.

from the diagrams that both IDA and PSS present a very low sensitivity to such variations, while FL shows a higher degree of sensitivity. This is justified because the latter strategy is based on canceling the nonlinearities and taking into consideration an exact knowledge of the model. Therefore, its performance is degraded because of parameter mismatches. However, it should be emphasized that this sensitivity is very low, and also that there are no signs of instability and a strong oscillation damping is still observed, even in presence of uncertainties.

5.2. Two-area four-machine test

In this section, a multimachine scenario is considered to assess the behavior of the nonlinear strategies. A two-area four-machine test is chosen for this purpose (see Fig. 10). Parameters of the system and controllers are taken from the mentioned example 12.6 [42]. AVR and governor (GOV) systems are installed in all generators, whereas oscillation damping controllers to be contrasted are placed in generators #1 and #3. The system transient response is analyzed performing a 300 ms three-phase fault at bus 8. To evaluate the performance and voltage regulation of the controller against a change in the topology network, one transmission line is opened immediately after the fault clearance (see breakers between buses 8 and 9 in Fig. 10).

Fig. 11 shows the generator load angles for the three cases under study: PSS, IDA, and FL controllers. There, it can be observed an increase in the oscillation damping when PSS are replaced by the nonlinear strategies. Fig. 11 also shows that the exponential behavior that FL control had in the single-machine test (see Fig. 6) is lost. This is due to the fact that the infinite-bus assumption is not valid any more in a weak multimachine power system. Nevertheless, the FL controller still presents the best oscillation damping when it is compared to PSS and IDA schemes. Fig. 12a–c shows the voltage profiles of the power system for all strategies. Controllers achieve a proper voltage regulation; however, a reduction in the stabilization time can be observed when nonlinear strategies are used. Finally, in Fig. 12d, the generator #1 terminal voltage is plotted before and after the fault. We can see that a good post-fault voltage regulation is accomplished by the strategies, confirming the correct value of the load angle reference calculated with the approach developed in Section 4.

6. FL versus IDA comparison

The philosophy behind FL control law is to transform a nonlinear system into a linear one to be able, in this way, to tune a high-performance controller. However, tuning for IDA gains are not systematic. Some guidelines to design its gains are presented in [34], but they seem to be more focused on keeping stability than in performance objectives (such as convergence speed, state decoupling, etc.). On the contrary, FL allows to design gains via well-known linear control techniques. As an example, FL-based adaptive control has been presented in power system control applications [31,48]. In [60], after applying FL, gains have been tuned via optimal control. Also, tuning via robust control techniques is proposed in [61]. This shows how flexible in designing its gains FL is. However, this feature has not been reported with IDA, where systematic designs for robust, optimal and adaptive versions are still in the stage of study.

However, in contrast with what has been discussed by some researchers, FL and IDA have many points in common. A better performance can be obtained with IDA if the α_1 design parameter, instead of being selected as constant, is considered state dependent [35]. Moreover, an interesting fact is that the following selection of α_1,

$$\alpha_1 = \left(\alpha_2 k_1 (x_1 - x_1^\star) + b_1 x_2\right)^{-1} \left(\alpha_2 k_1 x_3^\star - k_2 x_3 + + b_1 k_1 (\cos x_1 - \cos x_1^\star) + b_1 x_2 x_3 \cot x_1 + \left((b_2 P + v) - b_2^2 x_2\right) \csc x_1\right) \quad (63)$$

where

$$k_1 \triangleq b_3 + b_1 k_v, \quad (64)$$

$$k_2 \triangleq \alpha_2 b_3 + b_1 (b_2 + \alpha_2 k_v), \quad (65)$$

makes IDA to produce the same control law as the one obtained by FL. Therefore, the same law (performance, robustness, energy consumption, etc.) is obtained by both strategies when a particular selection of α_1 parameter is made.

7. Conclusions

A comparison among control strategies applied to synchronous generators were presented with the aim of damping oscillations in power systems. Controllers were tested for single-machine and multimachine scenarios and considering short circuits and parameter variations. It was seen that FL presents a better transient performance in the state variables, with excellent damping and a lesser stress to the actuator. IDA and PSS, in a slightly minor way, also had a very good performance. For demanding disturbances, the advantage of using nonlinear control strategies was evident against the use of PSS tuned at a determined operation point. Regarding strategy robustness, a very low sensitivity to variations in parameters was noticed for IDA and PSS, while in FL small deviations were observed. It can be broadly said that FL achieves a high performance because it is a kind of strategy based on canceling the model nonlinearities to obtain an input–output linear dynamics, and that makes necessary a detailed description of the system. On the other hand, IDA, being designed by considering the system total energy, loses performance in each of the individual states and presents a lower oscillation damping. As regards PSS controllers, disturbances or variations in load conditions might produce great deviations at the system operation point turning into invalid assumptions based on Taylor linearization.

The kind of nonlinear controller to be used will depend on the expected kind of damping, excitation system performance, knowledge of the power system model, etc. It can be regarded as an advantage that the considered PSS only needs the speed measurement (although some PSSs measure the generator terminal voltage and the generated electric power) while FL and IDA need to measure several generator states. However, this drawback can be overcome by including state observers (see for example [50,62,63]).

References

[1] Blaabjerg F, Chen Z, Kjaer S. Power electronics as efficient interface in dispersed power generation systems. IEEE Trans Power Electron 2004;19(5):1184–94.
[2] Colak I, Kabalci E, Bayindir R. Review of multilevel voltage source inverter topologies and control schemes. Energy Convers Manage 2011;52(2):1114–28.
[3] Leon AE, Amodeo SJ, Solsona JA, Valla MI. Non-linear optimal controller for unified power quality conditioners. IEEE Trans Power Electron 2011;4(4):435–46.
[4] Weimers L. HVDC Light: a new technology for a better environment. IEEE Power Eng Rev 1998;18(8):19–20.
[5] Leon AE, Solsona JA, Busada C, Chiacchiarini H, Valla MI. High-performance control of a three-phase voltage–source converter including feedforward compensation of the estimated load current. Energy Convers Manage 2009;50(8):2000–8.
[6] Rahimzadeh S, Bina MT. Looking for optimal number and placement of FACTS devices to manage the transmission congestion. Energy Convers Manage 2011;52(1):437–46.
[7] Hingorani NG, Gyugyi L. Understanding FACTS: concepts and technology of flexible AC transmission system. IEEE Press; 1999.
[8] Mahdad B, Bouktir T, Srairi K, Benbouzid ME. Dynamic strategy based fast decomposed GA coordinated with FACTS devices to enhance the optimal power flow. Energy Convers Manage 2010;51(7):1370–80.

[9] Singh BN, Chandra A, Al-Haddad K. DSP-based indirect-current-controlled STATCOM. Part II: Multifunctional capabilities. IEE Proc Electr Power Appl 2000;147(2):113–8.
[10] Leon AE, Mauricio JM, Solsona JA, Gomez-Exposito A. Software sensor-based STATCOM control under unbalanced conditions. IEEE Trans Power Deliev 2009;24(3):1623–32.
[11] Shakarami M, Kazemi A. Assessment of effect of SSSC stabilizer in different control channels on damping inter-area oscillations. Energy Convers Manage 2011;52(3):1622–9.
[12] Ara AL, Kazemi A, Niaki SN. Modelling of optimal unified power flow controller (OUPFC) for optimal steady-state performance of power systems. Energy Convers Manage 2011;52(2):1325–33.
[13] Asplund G, Eriksson K, Svensson K. HVDC Light-DC transmission based on voltage sourced converters. ABB Rev 1998;1:4–9.
[14] Ganapathy S, Velusami S. MOEA based design of decentralized controllers for LFC of interconnected power systems with nonlinearities, AC–DC parallel tie-lines and SMES units. Energy Convers Manage 2010;51(5):873–80.
[15] Flourentzou N, Agelidis VG, Demetriades GD. VSC-based HVDC power transmission systems: an overview. IEEE Trans Power Electron 2009;24(3):592–602.
[16] Carrasco JM, Franquelo LG, Bialasiewicz JT, Galvan E, Guisado RCP, Prats MAM, et al. Power-electronic systems for the grid integration of renewable energy sources: a survey. IEEE Trans Ind Electron 2006;53(4):1002–16.
[17] Amaris H, Alonso M. Coordinated reactive power management in power networks with wind turbines and FACTS devices. Energy Convers Manage 2011;52(7):2575–86.
[18] Melicio R, Mendes V, Catalao J. Fractional-order control and simulation of wind energy systems with PMSG/full-power converter topology. Energy Convers Manage 2010;51(6):1250–8.
[19] Mauricio JM, Leon AE, Gomez-Exposito A, Solsona JA. An adaptive nonlinear controller for DFIM-based wind energy conversion systems. IEEE Trans Energy Convers 2008;23(4):1025–35.
[20] Castillo-Cagigal M, Gutierrez A, Monasterio-Huelin F, Caamano-Martin E, Masa D, Jimenez-Leube J. A semi-distributed electric demand-side management system with PV generation for self-consumption enhancement. Energy Convers Manage 2011;52(7):2659–66.
[21] Vinothkumar K, Selvan M. Novel scheme for enhancement of fault ride-through capability of doubly fed induction generator based wind farms. Energy Convers Manage 2011;52(7):2651–8.
[22] Leon AE, Mauricio JM, Gomez-Exposito A, Solsona JA. An improved control strategy for hybrid wind farms. IEEE Trans Sustain Energy 2010;1(3):131–41.
[23] Alsayegh O, Alhajraf S, Albusairi H. Grid-connected renewable energy source systems: challenges and proposed management schemes. Energy Convers Manage 2010;51(8):1690–3.
[24] Andersson G, Donalek P, Farmer R, Hatziargyriou N, Kamwa I, Kundur P, et al. Causes of the 2003 major grid blackouts in North America and Europe, and recommended means to improve system dynamic performance. IEEE Trans Power Syst 2005;20(4):1922–8.
[25] Ilic MD, Allen H, Chapman JW, King CA, Lang JH, Litvinov E. Preventing future blackouts by means of enhanced electric power systems control: from complexity to order. Proc IEEE 2005;93(11):1920–41.
[26] Demello FP, Concordia C. Concepts of synchronous machine stability as affected by excitation control. IEEE Trans Power Apparat Syst 1969;88(4):316–29.
[27] Lu Q, Sun YZ. Nonlinear stabilizing control of multimachine systems. IEEE Trans Power Syst 1989;4(1):236–41.
[28] Chapman JW, Ilic MD, King CA, Eng L, Kaufman H. Stabilizing a multimachine power system via decentralized feedback linearizing excitation control. IEEE Trans Power Syst 1993;8(3):830–9.
[29] Wang Y, Hill DJ, Middleton RH, Gao L. Transient stability enhancement and voltage regulation of power systems. IEEE Trans Power Syst 1993;8(2):620–7.
[30] Akhrif O, Okou F-A, Dessaint L-A, Champagne R. Application of a multivariable feedback linearization scheme for rotor angle stability and voltage regulation of power systems. IEEE Trans Power Syst 1999;14(2):620–8.
[31] Kenne G, Goma R, Nkwawo H, Lamnabhi-Lagarrigue F, Arzande A, Vannier JC. An improved direct feedback linearization technique for transient stability enhancement and voltage regulation of power generators. Int J Electr Power Eng Syst 2010;32(7):809–16.
[32] Guo Y, Hill DJ, Wang Y. Global transient stability and voltage regulation for power systems. IEEE Trans Power Syst 2001;16(4):678–88.
[33] Bazanella AS, Kokotovic PV, e Silva AS. A dynamic extension for L_gV controllers. IEEE Trans Autom Control 1999;44(3):588–92.
[34] Galaz M, Ortega R, Bazanella AS, Stankovic AM. An energy-shaping approach to the design of excitation control of synchronous generators. Automatica 2003;39(1):111–9.
[35] Ortega R, Galaz M, Astolfi A, Sun Y, Shen T. Transient stabilization of multimachine power systems with nontrivial transfer conductances. IEEE Trans Autom Control 2005;50(1):60–75.
[36] Colbia-Vega A, de Leon-Morales J, Fridman L, Salas-Pena O, Mata-Jimenez M. Robust excitation control design using sliding-mode technique for multimachine power systems. Electr Power Syst Res 2008;78(9):1627–34.
[37] Al-Duwaish HN, Al-Hamouz ZM. A neural network based adaptive sliding mode controller: application to a power system stabilizer. Energy Convers Manage 2011;52(2):1533–8.
[38] Cabrera-Vázquez J, Loukianov AG, Cañedo JM, Utkin VI. Robust controller for synchronous generator with local load via VSC. Int J Electr Power Energ Syst 2007;29(4):348–59.
[39] Karimi A, Feliachi A. Decentralized adaptive backstepping control of electric power systems. Electr Power Syst Res 2008;78(3):484–93.
[40] Hardiansyah, Furuya S, Irisawa J. A robust H_∞ power system stabilizer design using reduced-order models. Int J Electr Power Energy Syst 2006;28(1):21–8.
[41] Kenne G, Goma R, Nkwawo H, Lamnabhi-Lagarrigue F, Arzande A, Vannier JC. Real-time transient stabilization and voltage regulation of power generators with unknown mechanical power input. Energy Convers Manage 2010;51(1):218–24.
[42] Kundur P. Power system stability and control. USA-New York: McGraw-Hill; 1994.
[43] Ortega R, Galaz-Larios M, Bazanella AS, Stankovic A. Excitation control of synchronous generators via total energy-shaping. Proc Am Control Conf 2001;2:817–22.
[44] Khalil H. Nonlinear systems. 2nd ed. Prentice-Hall; 1996.
[45] Ortega R, van der Schaft A, Maschke B, Escobar G. Interconnection and damping assignment passivity-based control of port-controlled hamiltonian systems. Automatica 2002;38(4):585–96.
[46] Zhu C, Zhou R, Wang Y. A new decentralized nonlinear voltage controller for multimachine power systems. IEEE Trans Power Syst 1998;13(1):211–6.
[47] Wang Y, Xie L, Hill DJ, Middleton RH. Robust nonlinear controller design for transient stability enhancement of power systems. In: Proceedings of the 31st IEEE conference on decision and control, vol. 1, 1992, pp. 1117–22.
[48] Wang Y, Hill DJ, Middleton RH, Gao L. Transient stabilization of power systems with an adaptive control law. Automatica 1994;30(9):1409–13.
[49] Mak FK. Design of nonlinear generator exciters using differential geometric control theories. In: Proceedings of the 31st IEEE conference on decision and control, vol. 1, 1992, pp. 1149–53.
[50] Jiang L, Wu QH, Zhang C, Zhou XX. Observer-based nonlinear control of synchronous generators with perturbation estimation. Int J Electr Power Energy Syst 2001;23(5):359–67.
[51] Karimi A, Feliachi A. Decentralized extended-backstepping control of power systems. IEEE Power Eng Soc Gen Meet 2006:1–8.
[52] Cao Y, Jiang L, Cheng S, Chen D, Malik OP, Hope GS. A nonlinear variable structure stabilizer for power system stability. IEEE Trans Energy Convers 1994;9(3):489–95.
[53] Zaborszky J, Whang K-W, Prasad K. Stabilizing control in emergencies. Part 1. Equilibrium point and state determination. IEEE Trans Power Apparat Syst 1981;100(5):2374–80.
[54] Rerkpreedapong D, Feliachi A. Decentralized control of nonlinear electric power systems thru excitation and governor systems using local measurements and feedback linearization. Proc 43rd IEEE Midwest Symp Circuits Syst 2000;2:626–9.
[55] Wu J, Yokoyama A, Lu Q, Goto M, Konishi H. Decentralised nonlinear equilibrium point adaptive control of generators for improving multimachine power system transient stability. IEE Proc Gen Transm Distrib 2003;150(6):697–708.
[56] Fan L, Feliachi A. Decentralized stabilization of nonlinear electric power systems using local measurements and feedback linearization. Proc 43rd IEEE Midwest Symp Circuits Syst 2000;2:638–41.
[57] Lahdhiri T, Alouani AT. Nonlinear excitation control of a synchronous generator with implicit terminal voltage regulation. Electr Power Syst Res 1996;36(2):101–12.
[58] Okou F, Dessaint L-A, Akhrif O. Power systems stability enhancement using a wide-area signals based hierarchical controller. IEEE Trans Power Syst 2005;20(3):1465–77.
[59] Zhang K, Dai X. Strict decentralized nonlinear controller for synchronous generator set. IEEE Power India Conf 2006:1–8.
[60] Lu Q, Sun Y, Xu Z, Mochizuki T. Decentralized nonlinear optimal excitation control. IEEE Trans Power Syst 1996;11(4):1957–62.
[61] Wang Y, Guo G, Hill DJ. Robust decentralized nonlinear controller design for multimachine power systems. Automatica 1997;33(9):1725–33.
[62] Rakhshani E, Sadeh J. Practical viewpoints on load frequency control problem in a deregulated power system. Energy Convers Manage 2010;51(6):1148–56.
[63] Leon-Morales JD, Busawon K, Acha-Daza S. A robust observer-based controller for synchronous generators. Int J Electr Power Energy Syst 2001;23(3):195–211.